Efficient Computation of Transition State Resonances and Reaction Rates from a Quantum Normal Form

Roman Schubert, Holger Waalkens, and Stephen Wiggins
School of Mathematics, University Walk, University of Bristol, Bristol BS8 1TW, United Kingdom
(Received 12 October 2005; published 2 June 2006)

A quantum version of a recent formulation of transition state theory in *phase space* is presented. The theory developed provides an algorithm to compute quantum reaction rates and the associated Gamov-Siegert resonances with very high accuracy. The algorithm is especially efficient for multi-degree-of-freedom systems where other approaches are no longer feasible.

DOI: 10.1103/PhysRevLett.96.218302 PACS numbers: 82.20.Ln, 05.45.−a, 34.10.+x

Introduction.—The question of how, as Marcus [1] formulates it, a system ''skis the reaction slope'' is one of the crucial questions in reaction dynamics. Experimental techniques like photodissociation of jet-cooled molecules, molecular beam experiments, or transition state spectroscopy give detailed information about the reaction process as has recently been demonstrated, e.g., for the ''paradigm'' reaction of hydrogen atom-diatom collisions (see, e.g., the review paper [2]). A chemical reaction can often be viewed as the scattering problem across a saddle point of the interaction potential. The cumulative reaction probability is then given by

$$N(E) = \mathrm{tr}\hat{t}\hat{t}^\dagger = \sum_{n_r,n_p} |\langle \psi^{\mathrm{out}}_{n_p}|\hat{S}|\psi^{\mathrm{in}}_{n_r}\rangle|^2,$$

where $\hat{t}$ is the transmission subblock of the scattering operator $\hat{S}$ for energy E and the summation in the latter expression runs over all incoming reactant states with quantum numbers n_r and outgoing product states with quantum numbers n_p. The *ab initio* quantum mechanical computation of $N(E)$ soon becomes very expensive if the number of atoms in the system increases beyond 3 and one has to resort to suitable approximations. The main approach to compute $N(E)$ *classically* is transition state theory which was invented by Eyring, Polanyi, and Wigner in the 1930's. The main idea is to define a dividing surface that divides the energy surface into a reactant and a product component and compute the rate from the directional phase space flux through this surface. In order not to overestimate the rate, the dividing surface must not be recrossed by reactive trajectories. In the 1970's Pechukas, Pollak, and others [3] showed that for 2 degrees of freedom such a dividing surface can be constructed from a periodic orbit (the so-called periodic orbit dividing surface). Recently, it has been shown that in higher dimension a dividing surface that is free of recrossings can be built from a normally hyperbolic invariant manifold (NHIM) [4]. The dividing surface and the NHIM can be directly constructed from an algorithm based on a Poincaré-Birkhoff normal form procedure [5] which also gives an expression for the flux [6].

Much effort has been devoted to developing a quantum version of transition state theory whose implementation remains feasible for multidimensional systems (see the flux-flux autocorrelation function formalism by Miller and co-workers [7]). In this Letter we present a quantum version of the normal form procedure that lead to the construction of the high-dimensional phase space structures that govern the classical reaction dynamics (see [8] for work in a similar direction). We demonstrate that this quantum normal form approach to transition state theory provides an efficient procedure to compute quantum reaction rates and the corresponding Gamov-Siegert resonances [9].

The quantum normal form.—We consider scattering across a *single* equilibrium point of saddle-center-???-center stability type (''saddle'' for short), i.e., the matrix associated with the linearized classical equations of motion has one pair of real eigenvalues $\pm\lambda$ associated with the saddle or ''reaction coordinate'' and $f-1$ pairs (f being the number of degrees of freedom) of imaginary eigenvalues $\pm i\omega_k$, $k = 2, \ldots, f$, associated with the center or ''bath'' degrees of freedom. The main idea of which the seed can already be found, e.g., in [10] in the chemical and [11] in the mathematical literature, is to derive a local approximation of the Hamilton operator of the scattering problem that is valid near the saddle, and in order to facilitate further computations, takes a much simpler form than the original Hamiltonian. We therefore develop an explicit algorithm to realize the ideas of [11] based on the Wigner-Weyl calculus that has been used by others before to compute energy spectra associated with stable equilibria [12]. Here the manipulations of an operator $\hat{A}$ are expressed in terms of its *symbol*, which is the function $A(p, x)$ defined by

$$\hat{A}\psi(x) = \frac{1}{(2\pi\hbar)^f}\int_{R^{2f}} e^{i\langle x-y,p\rangle/\hbar} A\left(p, \frac{x+y}{2}\right)\psi(y)dydp.$$

Defining the multiplication $*$ of two symbols A and B as

$$A * B = A\exp\left(i\frac{\hbar}{2}[\langle \overleftarrow{\partial}_x, \overrightarrow{\partial}_p\rangle - \langle \overrightarrow{\partial}_x, \overleftarrow{\partial}_p\rangle]\right)B, \qquad (1)$$

where the arrows indicate whether the partial differentiation acts to the left (on A) or to the right (on B), gives the property that the quantization of the product of two symbols A and B is equal to the product of the quantizations of the individual symbols, i.e., $\hat{A}\hat{B} = \widehat{A * B}$. The $*$ product leads to the definition of the Moyal brackets

$$\{A, B\}_M = \frac{i}{\hbar}(A * B - B * A).$$

We define the *order* s of a monomial $p^\alpha x^\beta \hbar^n \equiv p_1^{\alpha_1} \cdots p_f^{\alpha_f} x_1^{\beta_1} \cdots x_f^{\beta_f} \hbar^n$ according to $s = |\alpha| + |\beta| + 2n \equiv \alpha_1 + \cdots + \alpha_f + \beta_1 + \cdots + \beta_f + 2n$, and denote the vector space of polynomials spanned by monomials of order s by $\mathcal{W}_s$. For $A \in \mathcal{W}_s$ and $B \in \mathcal{W}_{s'}$ we define the Moyal adjoint by $\mathrm{Mad}_A B := \{A, B\}_M$, then its iterates satisfy $[\mathrm{Mad}_A]^n B \in \mathcal{W}_{n(s-2)+s'}$.

The symbol of the Hamilton operator $\hat{H}$ can be expanded about the saddle according to

$$H = E_0 + \sum_{s=2}^{\infty} H_s, \tag{2}$$

where E_0 is a constant energy and $H_s \in \mathcal{W}_s$. Like in the classical case [5], a suitable linear canonical transformation allows one to write the second order term as

$$H_2 = \lambda I + \omega_2 J_2 + \cdots + \omega_f J_f$$

with $I = p_1 x_1$, $J_k = \frac{1}{2}(p_k^2 + x_k^2)$, $k = 2, \ldots, f$. Note that $p_1 x_1 = (\tilde{p}_1^2 - \tilde{q}_1^2)/2$, where (p_1, x_1) and $(\tilde{p}_1, \tilde{q}_1)$ are related by a rotation of 45°.

In order to simplify the Hamiltonian $\hat{H}$ we will transform it by successive conjugations with unitary operators, $\hat{H} =: \hat{H}^{(2)} \to \hat{H}^{(3)} \to \hat{H}^{(4)} \to \cdots \to \hat{H}^{(N)}$, where

$$\hat{H}^{(n)} = e^{i\hat{W}_n/\hbar} \hat{H}^{(n-1)} e^{-i\hat{W}_n/\hbar},$$

with $W_n \in \mathcal{W}_n$. Using the Moyal adjoint the symbol of the right-hand side can be expanded as

$$H^{(n)} = \sum_{k=0}^{\infty} \frac{1}{k!} [\mathrm{Mad}_{W_n}]^k H^{(n-1)}. \tag{3}$$

If we expand furthermore each of the symbols $H^{(n)}$ in a power series as in (2), $H^{(n)} = E_0 + \sum_{s \geq 2} H_s^{(n)}$, with $H_s^{(n)} \in \mathcal{W}_s$, then using (3) the terms in these series can be related by

$$H_s^{(n)} = \sum_{k=0}^{[(s-2)/(n-2)]} \frac{1}{k!} [\mathrm{Mad}_{W_n}]^k H_{s-k(n-2)}^{(n-1)},$$

where $[\cdot]$ denotes the integer part. Notice that for $s < n$, $H_s^{(n)} = H_s^{(n-1)}$, and for $s = n$ we obtain

$$H_n^{(n)} = H_n^{(n-1)} + \{W_n, H_2\}, \tag{4}$$

where we have used that $H_2^{(n)} = H_2$ for all $n \geq 3$ and that the Moyal brackets reduces to the Poisson brackets $\{\cdot, \cdot\}$ if one of its arguments is a quadratic function. This is the homological equation which is familiar from the classical normal form algorithm, [5], and under the nonresonance conditions on the frequencies ω_k, given any $H_n^{(n-1)} \in \mathcal{W}_n$ there exists a unique $W_n \in \mathcal{W}_n$ such that $H_n^{(n)}$ can be written as a function of $I, J_2, \ldots, J_f$ alone.

Choosing the generators of the unitary transformations W_n recursively for $n = 3, 4, \ldots N$ as solutions of (4) we obtain an operator $\hat{H}^{(N)}$ whose symbol is of the form $H^{(N)} = E_0 + \sum_{s=2}^{N} H_s^{(N)} + R^{(N+1)}$, where the first part is a polynomial in $I, J_2, \ldots, J_f$, i.e., is in *normal form*, and the remainder $R^{(N+1)}$ consists of terms of order $N + 1$ and higher. In a final step we want to express the quantization of the normal form part as an operator function of the quantized $\hat{I}$ and $\hat{J}_k$. To this end we use a recursion relation for $\hat{I}^n$ (and a similar one for the J_k), $\hat{I}^{n+1} = \hat{I}\hat{I}^n - \hat{I}^{n-1} n^2 \hbar^2/4$, which can be derived from the product formula (1). This allows us to express quantizations of powers of I as a polynomial in powers of $\hat{I}$. In this way we find a polynomial $H_{\mathrm{QNF}}^{(N)}$ such that

$$U_N^* \hat{H} U_N = H_{\mathrm{QNF}}^{(N)}(\hat{I}, \hat{J}_2, \ldots, \hat{J}_f) + \hat{R}^{(N+1)},$$

where $U_N = \prod_{n=3}^{N} e^{-i\hat{W}_n/\hbar}$. $H_{\mathrm{QNF}}^{(N)}(\hat{I}, \hat{J}_2, \ldots, \hat{J}_f)$ is called the quantum normal form (QNF) of $\hat{H}$ of order N. The remainder term $\hat{R}^{(N+1)}$ has a symbol which is of order $N + 1$ and is therefore very small near the saddle point. Hence the dynamics near the saddle point can be described with high accuracy by the QNF Hamiltonian. The QNF Hamiltonian is an operator function of the commuting operators $\hat{I}$ and $\hat{J}_k$ whose properties are well understood.

In the limit $\hbar \to 0$ we recover the classical normal form of order N. The classical normal form gives *explicit* ex-

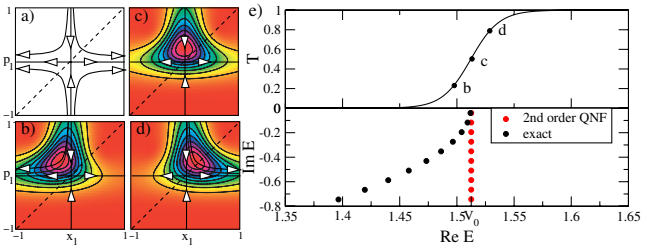

FIG. 1 (color online). (a) Normal form saddle plane (x_1, p_1) with the projection of the NHIM ($x_1 = p_1 = 0$), its stable and unstable manifolds ($x_1 = 0$ and $p_1 = 0$, respectively), the dividing surface ($p_1 = x_1$; dashed line) separating reactants ($p_1 > x_1$) from products ($p_1 < x_1$), forward and backward reactive trajectories that have $E > E_0$ (hyperbola with branches in the first and third quadrant, respectively) and nonreactive trajectories that have $E < E_0$ (hyperbola with branches in the second and fourth quadrant). (b),(c),(d) show Husimi representations [13] of the scattering state $\psi_{\mathrm{react}}^{\mathrm{in}}$ for the energies marked in (e). (e) Transmission probability $T(E)$ and Gamov-Siegert resonances in the complex energy plane for the Eckart potential. The parameters are $a = 1$, $10A = B = 5$, $m = 1$, and $\hbar = 0.1$.

pressions for the NHIM, its stable and unstable manifolds and the dividing surface that govern the classical dynamics [5] [see Fig. 1(a)].

Resonances and reaction rates.—The eigenfunctions of the QNF Hamiltonian are tensor products of harmonic oscillator wave functions for the center degrees of freedom x_k, $k = 2, \ldots, f$, and eigenfunctions of the operator

$$\hat{I} = \frac{\hbar}{i}\left(x_1 \partial_{x_1} + \frac{1}{2}\right)$$

associated with the saddle direction. The operator $\hat{I}$ has eigenfunctions [13]

$$\psi^{\text{out}}_{\text{react/prod}}(x_1) = \Theta(\mp x_1) x_1^{-1/2 + iI/\hbar},$$

Θ being the step function, which are outgoing waves. Incoming waves can be defined from the Fourier transforms

$$\psi^{\text{in}}_{\text{react/prod}}(x_1) = \frac{1}{\sqrt{2\pi\hbar}} \int \psi^{\text{out}*}_{\text{prod/react}}(y_1) e^{ix_1 y_1/\hbar} dy_1. \quad (5)$$

For $I > 0$ these wave functions are associated with the reactants and products pieces of the forward and backward trajectories in Fig. 1(a) [13]. Expressing the functions $\psi^{\text{in}}_{\text{react/prod}}$ in terms of $\psi^{\text{out}}_{\text{react/prod}}$ gives the entries of a local S matrix:

$$\psi^{\text{in}}_{\text{prod}} = S_{n11}\psi^{\text{out}}_{\text{prod}} + S_{n21}\psi^{\text{out}}_{\text{react}},$$
$$\psi^{\text{in}}_{\text{react}} = S_{n12}\psi^{\text{out}}_{\text{prod}} + S_{n22}\psi^{\text{out}}_{\text{react}}.$$

Here, n denotes the vector $(n_2, \ldots, n_f)$ of quantum numbers of the modes in the center directions. The local S matrix is block diagonal. Mode mixing is a "global" effect which occurs from connecting the local wave functions to the asymptotic reactants' and products' wave functions. However, the local S matrix alone already contains the full information needed to compute reaction rates and resonances (if the NHIM is the only trapped set [11]).

Evaluating the integrals (5) gives

$$S_n(E) = \frac{e^{i(\pi/4 - I\ln\hbar/\hbar)}}{\sqrt{2\pi}} \Gamma\left(\frac{1}{2} - i\frac{I}{\hbar}\right) \times \begin{pmatrix} -ie^{-(\pi/2)(I/\hbar)} & e^{(\pi/2)(I/\hbar)} \\ e^{(\pi/2)(I/\hbar)} & -ie^{-(\pi/2)(I/\hbar)} \end{pmatrix}$$

with I being implicitly defined by

$$H^{(N)}_{\text{QNF}}(I, \hbar(n_2 + 1/2), \ldots, \hbar(n_f + 1/2)) = E. \quad (6)$$

The transmission probability of mode n is

$$T_n(E) = |S_{n12}(E)|^2 = (1 + e^{-2\pi(I/\hbar)})^{-1},$$

which gives the cumulative reaction probability $N(E) = \sum_n T_n(E)$. The S matrix has poles at $I = -i\hbar(n_1 + 1/2)$ for non-negative integers n_1 and these define the Gamov-Siegert resonances via (6).

Examples.—For 1D potential barriers, i.e., Hamiltonians of the form $H = p^2/(2m) + V(x)$, where $V(x)$ has a maximum which we can assume to be at $x = 0$, the second order QNF is easily obtained and gives the well-known result $\hat{H}_{\text{QNF},2} = V(0) + \lambda\hat{I}$ with $\lambda = [-V''(0)/m]^{1/2}$, which is equivalent to approximating the potential barrier by an inverted parabola. The first nontrivial correction to this result comes from the fourth order QNF $\hat{H}_{\text{QNF},4}$ given by

$$V(0) + \lambda\hat{I} + \frac{1}{16m^2\lambda^2}\left\{\frac{5}{3m\lambda^2}[V'''(0)]^2 + V''''(0)\right\}\hat{I}^2 - \frac{1}{64m^2\lambda^2}\left\{\frac{7}{9m\lambda^2}[V'''(0)]^2 + V''''(0)\right\}\hbar^2.$$

We apply the QNF to the Eckart potential [14]

$$V_{\text{Eckart}}(x) = A\frac{e^{(x+x_0)/a}}{1 + e^{(x+x_0)/a}} + B\frac{e^{(x+x_0)/a}}{(1 + e^{(x+x_0)/a})^2}$$

with $x_0 = a\ln(B + A)/(B - A)$ and $B > A \geq 0$. Figure 1 shows the exact transmission probability which is known analytically, and the exact string of resonances together with the resonances from the second order QNF which have constant imaginary part. The bending of the string of exact resonances is a nonlinear effect that is very well described already by the fourth order QNF. The excellent accuracy of the resonances and the cumulative reaction probability computed from higher orders of the QNF is illustrated in Fig. 2.

We next consider the three-degree-of-freedom example of a Hamiltonian with an Eckart potential in the x_1 direction, and Morse potentials

$$V_{\text{Morse};k}(x_k) = D_{e;k}(e^{-2\alpha_k x_k} - 2e^{-\alpha_k x_k}), \qquad k = 2, 3$$

in the x_2 direction and x_3 direction, plus a mutual kinetic coupling $\epsilon(p_1p_2 + p_1p_3 + p_2p_3)$. In Fig. 3 the cumulative reaction probability and the resonances computed from the QNF are compared with the exact results. In the uncoupled case $\epsilon = 0$, $N(E)$ increases as a function of E at integer steps each time a new transition channel opens, i.e., when

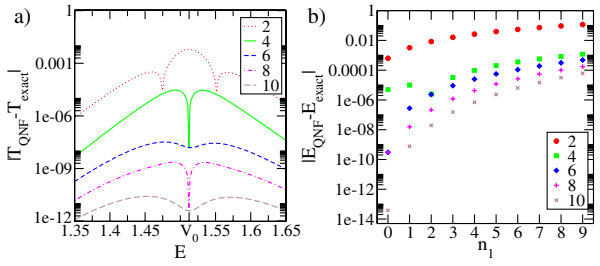

FIG. 2 (color online). (a) Errors for the transmission probability of the Eckart potential computed from the QNF. (b) Differences between the QNF resonances and the corresponding exact complex energies of the Eckart potential as a function of the quantum number n_1. The different colors correspond to different orders of the QNF. The parameters are the same as in Fig. 1.

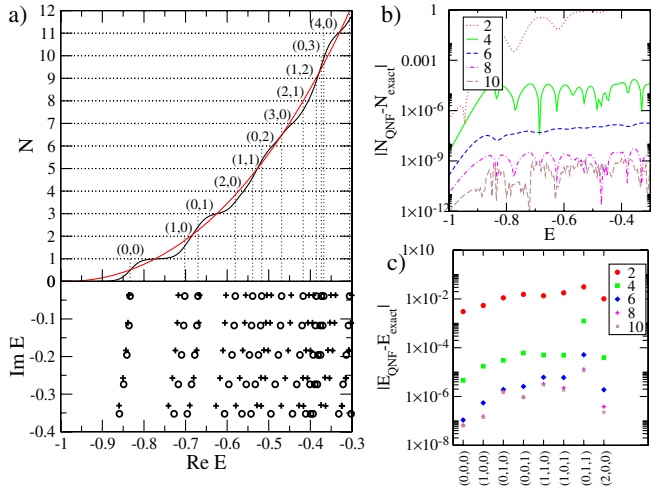

FIG. 3 (color online). (a) The top panel shows the cumulative reaction probability $N(E)$ (oscillatory curve) and the classical flux computed according to [6] divided by $(2\pi\hbar)^2$ (smooth curve) for the Eckart-Morse-Morse potential defined in the text with $\epsilon = 0$. It also shows the quantum numbers (n_2, n_3) of the Morse oscillators that contribute to the quantization steps. The bottom panel shows the resonances in the complex energy plane marked by circles for the uncoupled case $\epsilon = 0$ and by crosses for the strongly coupled case $\epsilon = 0.3$. For the coupled case the numerically exact resonances are computed from the complex dilation method [15]. The parameters for the Eckart potential are the same as in Fig. 1. The parameters for the Morse potential are $D_{e;1} = 1$, $D_{e;2} = 3/2$, $\alpha_1 = 1$, and $\alpha_2 = 1$. Again we choose $m = 1$ and $\hbar = 0.1$. (b) Errors for the cumulative reaction probability in (a) for different orders of the QNF. (c) Errors for a selection of resonances (n_1, n_2, n_3) computed from the QNF for the coupled case $\epsilon = 0.3$.

the transmission probability $T_{(n_2,n_3)}(E)$ of a mode (n_2, n_3) of the two Morse oscillators switches from 0 to 1. For both the uncoupled and strongly coupled case the resonances form a distorted lattice parametrized by the mode quantum numbers (n_2, n_3) in the horizontal direction and the quantum number n_1 in the vertical direction. Similar to the 1D example, each string of constant (n_2, n_3) is related to one step of $N(E)$. Like in the 1D case the agreement of the QNF results with the exact results is excellent and this remains the case even for the strongly coupled system. The QNF is an asymptotic expansion which in general does not converge. However, up to the maximal order shown the accuracy of the QNF results still increases as the order of the QNF is increased.

Conclusions.—The QNF computation of reaction probabilities and the corresponding Gamov-Siegert resonances is highly promising since it opens the way to study high-dimensional systems for which other techniques based on the *ab initio* solution of the quantum scattering problem like the complex dilation method [15] or the utilization of an absorbing potential [16] are no longer feasible. In fact, in order to compute sufficiently accurate resonances from the complex dilation method that facilitate a comparison for our QNF computations for the shown three-degree-of-freedom example, we had to diagonalize matrices of size 2500×2500 reaching the limits of our computation power. However, the numerical effort for computing the QNF is only slightly higher than the effort for computing the classical normal form (NF). The main difference is that the Poisson brackets in the classical NF needs to be replaced by the Moyal brackets. Moreover, the QNF gives an explicit formula for the resonances from which they can be computed directly by inserting the corresponding quantum numbers. This leads to a direct assignment of the resonances. The QNF provides a quantum version of transition state theory that, in the classical limit, is in accord with the classical phase structures that govern the reaction dynamics. In fact, the classical phase space structures form the skeleton for the scattering and resonance wave functions, and exploiting this relationship is the subject of our future studies.

[1] R. A. Marcus, Science **256**, 1523 (1992).
[2] R. T. Skodje and X. Yang, Int. Rev. Phys. Chem. **23**, 253 (2004).
[3] P. Pechukas and F. J. McLafferty, J. Chem. Phys. **58**, 1622 (1973); P. Pechukas and E. Pollak, J. Chem. Phys. **69**, 1218 (1978).
[4] S. Wiggins, Physica D (Amsterdam) **44**, 471 (1990); S. Wiggins, L. Wiesenfeld, C. Jaffé, and T. Uzer, Phys. Rev. Lett. **86**, 5478 (2001).
[5] T. Uzer, C. Jaffé, J. Palacián, P. Yanguas, and S. Wiggins, Nonlinearity **15**, 957 (2002); H. Waalkens, A. Burbanks, and S. Wiggins, J. Chem. Phys. **121**, 6207 (2004).
[6] H. Waalkens and S. Wiggins, J. Phys. A **37**, L435 (2004).
[7] W. H. Miller, J. Phys. Chem. A **102**, 793 (1998).
[8] S. C. Creagh, Nonlinearity **17**, 1261 (2004); **18**, 2089 (2005).
[9] R. S. Friedman and D. G. Truhlar, Chem. Phys. Lett. **183**, 539 (1991); T. Seideman and W. H. Miller, J. Chem. Phys. **95**, 1768 (1991).
[10] R. Hernandez and W. H. Miller, Chem. Phys. Lett. **214**, 129 (1993); R. Hernandez, J. Chem. Phys. **101**, 9534 (1994).
[11] J. Sjöstrand, Asymptotic Analysis **36**, 93 (2003); N. Kaidi and P. Kerdelhué, *ibid.* **23**, 1 (2000).
[12] L. E. Fried and G. S. Ezra, J. Chem. Phys. **92**, 3144 (1988); P. Crehan, J. Phys. A **23**, 5815 (1990).
[13] Y. Colin de Verdière and B. Parisse, Commun. Partial Differ. Equ. **19**, 1535 (1994); Ann. Inst. Henri Poincaré A, Phys. Théor. **61**, 347 (1994); Commun. Math. Phys. **205**, 459 (1999); S. Nonnenmacher and A. Voros, J. Phys. A **30**, 295 (1997).
[14] C. Eckart, Phys. Rev. **35**, 1303 (1930).
[15] N. Moiseyev, Phys. Rep. **302**, 212 (1998); W. P. Reinhardt, Annu. Rev. Phys. Chem. **33**, 223 (1982); B. Simon, Phys. Lett. A **71**, 211 (1979).
[16] A. Neumaier and V. A. Mandelshtam, Phys. Rev. Lett. **86**, 5031 (2001).